Unfolding and Refolding of the Glutamine-Binding Protein from *Escherichia coli* and Its Complex with Glutamine Induced by Guanidine Hydrochloride†

Maria Staiano,‡ Viviana Scognamiglio,‡ Mose' Rossi,‡ Sabato D'Auria,*,‡ Olga V. Stepanenko,§ Irina M. Kuznetsova,§ and Konstantin K. Turoverov*,§

Institute of Protein Biochemistry, CNR, Naples, Italy, and Institute of Cytology, Russian Academy of Sciences, St. Petersburg, Russia

Received October 8, 2004; Revised Manuscript Received February 21, 2005

ABSTRACT: The aim of this work was to study the conformational changes of the *Escherichia coli* glutamine-binding protein (GlnBP) induced by GdnHCl and the effect of the binding of glutamine (Gln) on these processes. To this end, GdnHCl-induced unfolding of GlnBP alone and its GlnBP−Gln complex was studied by protein intrinsic fluorescence, ANS emission fluorescence, and far- and near-UV circular dichroism spectroscopy. The obtained spectroscopic data were interpreted taking into the account the peculiarities of protein three-dimensional structure. In particular, the fact that formation of a complex of GlnBP and Gln, which essentially changes the global structure of protein, affects only insignificantly the microenvironments of tryptophan residues elucidates the similarity of the emission spectra of GlnBP and the GlnBP−Gln complex, and the existence of quenching groups near tyrosine residues and an effective nonradiative Tyr → Trp and/or Tyr → Tyr → Trp energy transfer provide an explanation for the negligibly small contribution of tyrosine to the bulk fluorescence of the native protein and for its increase in protein unfolding. The use of the parametric presentation of fluorescence data showed that both GlnBP unfolding and GlnBP−Gln unfolding are three-step processes ($N \rightarrow I_1 \rightarrow I_2 \rightarrow U$), though in the case of the GlnBP−Gln complex these stages essentially overlap. Despite the complex character, GlnBP unfolding is completely reversible. The dramatic shift of the $N \rightarrow I_1$ process to higher GdnHCl concentrations for the GlnBP−Gln complex in comparison with GlnBP was shown.

The question of how a protein folds into its unique, compact, highly ordered, and functionally active form is one of the most intriguing and perplexing questions of structural and cellular biology (*1*−*10*). The field of protein folding has seen essential advances in recent years because of growing interest in diseases that result from protein misfolding and aggregation (*11*−*15*).

The majority of investigations have been done on small single-domain proteins. This work is focused on the processes of folding and unfolding of GlnBP[1] from *Escherichia coli*, which is a monomer (25 kDa) consisting of two globular domains (termed large and small), which exhibit a similar supersecondary structure (*16*). The small domain consists of three α-helices and four parallel and one antiparallel *β*-strands connected by a large loop, while the large domain contains two extra α-helices and three *β*-strands. The domains are linked by two antiparallel *β*-strands. The deep cleft formed between the domains contains the ligand-binding site (Figure 1). GlnBP from *E. coli* is responsible for the first step in the active transport of L-glutamine across the cytoplasmic membrane. Differences in the structures of the ligand-bound and ligand-free proteins make GlnBP a good candidate for a biological recognition element in the development of a biosensor (*21*, *22*). The study of partially folded intermediate states of proteins is important in view of the assumption of their functional role in living cells (*23*). In particular for GlnBP, it can be important for elucidating the mechanism of ligand release on the surface of membranes.

In this work, the GdnHCl-induced unfolding−refolding processes of GlnBP from *E. coli* in the absence and presence of Gln were studied by several physicochemical methods and especially by the intrinsic fluorescence of the protein. This method is a powerful tool for examining structure, dynamics, and folding−unfolding processes of proteins (*24*−*29*) because of the high sensitivity of various parameters of the fluorescence of tryptophan residues (spectrum position, quantum yield, fluorescence anisotropy, etc.) to their microenvironment and to the peculiarities of their location in protein macromolecules. Along with tryptophan fluorescence, the change in tyrosine fluorescence upon protein folding and

† This project was realized in the frame of CRdC-ATIBB POR UE-Campania Mis 3.16 activities (S.D. and M.R.). This work was supported by grants from FIRB (S.D. and M.R.), the Italian National Research Council (S.D, and M.R.), INTAS 2001-2347 (K.K.T.), INTAS 04-83-3162 (O.V.S.), RFBR 05-04-48588 (O.V.S.), and the Presidium of the Russian Academy of Sciences for the program "Molecular and Cell Biology" (K.K.T.).

* To whom correspondence should be addressed. S.D.: Institute of Protein Biochemistry, Via P. Castellino, 111 80131 Naples, Italy; phone, +39-0816132250; fax, +39-0816132277; e-mail, s.dauria@ibp.cnr.it. K.K.T.: Institute of Cytology, Russian Academy of Sciences, Tikhoretsky av., 4, 194064 St. Petersburg, Russia; phone, 7(812) 247-1957; fax, 7(812) 247-0341; e-mail, kkt@mail.cytspb.rssi.ru.

‡ CNR.

§ Russian Academy of Sciences.

[1] Abbreviations: Gln, glutamine; GlnBP, glutamine-binding protein; GlnBP−Gln, complex of glutamine-binding protein with glutamine; GdnHCl, guanidine hydrochloride; ANS, 1-anilinonaphthalene-8-sulfonic acid; CD, circular dichroism.

10.1021/bi0478300 CCC: $30.25
Published on Web 03/25/2005

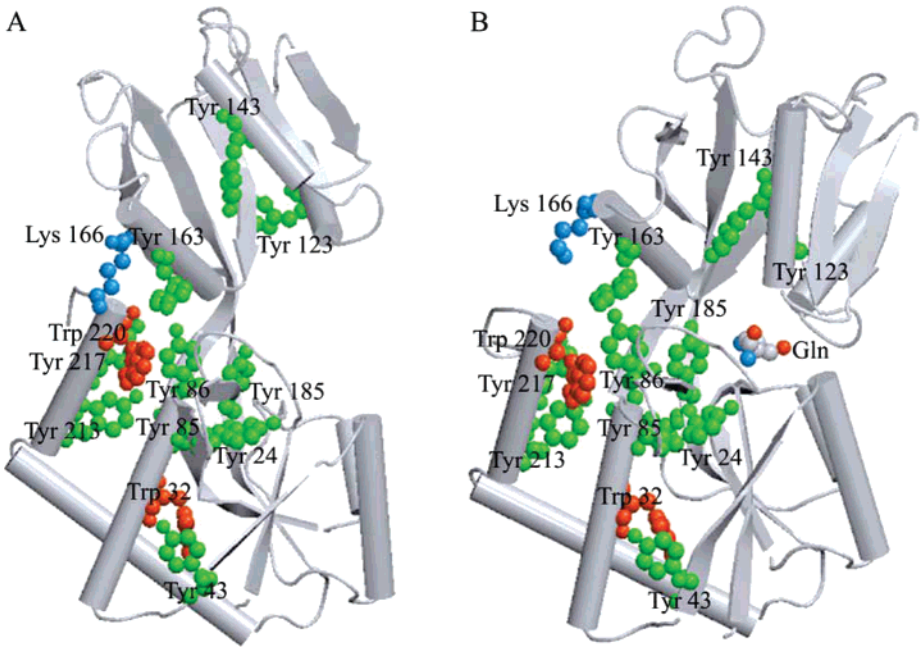

FIGURE 1: Spatial pattern of GlnBP (A) and its complex with Gln (B). The backbone of the molecule is represented as a cartoon diagram; tryptophan residues (red), tyrosine residues (green), Lys 166 (blue) belonging to microenvironment of Trp 220, and Gln are shown as spheres. Complex formation results in the collapse of the protein macromolecule around Gln, resulting in cleft closure. This figure was constructed using Protein Data Bank (*18*) entries 1GGG (*16*) and 1WDN (*17*). The drawing was generated with VMD (*19*) and Raster3D (*20*).

unfolding was also recorded. The advantages of the use of fluorescence emission of tyrosine residues are their multiplicity and uniform distribution in the protein molecule. Analysis of fluorescence experimental data was performed in parallel with the analysis of tryptophan and tyrosine residue microenvironment on the basis of GlnBP three-dimensional (3D) structure.

Our data show that though there are two intermediate partially folded states on the pathway of GlnBP unfolding this process is reversible and refolding goes via the same intermediate states. It is also shown that formation of a complex with Gln results in an essential increase in the resistance of GlnBP to the denaturation action of GdnHCl. In fact, the transition from the native to partially folded state I_1 for GlnBP−Gln takes place at higher GdnHCl concentrations than for GlnBP alone.

MATERIALS AND METHODS

Preparations. The glutamine-binding protein from *E. coli* was prepared and purified according to the method of ref *21*. L-Glutamine was obtained from Sigma. All the other chemicals used were commercial samples of the purest quality. The protein concentration was determined by the method of Bradford (*30*) with bovine serum albumin as the standard on a double-beam Cary 1E spectrophotometer (Varian, Mulgrade, Victoria, Australia). The protein concentration was 0.1−0.3 mg/mL. For complex formation, 10^{-3}−10^{-2} M Gln was added. In all experiments, 10 mM Tris-HCl buffer (pH 8.5) was used. GdnHCl (Nacalai Tesque, Japan) was used without additional purification. The GdnHCl concentration was determined by refraction index with an Abbe refractometer (LOMO).

Analysis of Protein 3D Structure. The location of tryptophan and tyrosine residues in GlnBP and the complex of GlnBP with Gln was analyzed according to the atom coordinates of the crystal structure of GlnBP (PDB entry 1GGG; *16*) and the complex with Gln (PDB entry 1WDN; *17*). The microenvironment of the tryptophan or tyrosine residue was determined as a set of atoms located some distance less than r_0 from the geometrical center of the indole or phenol ring; r_0 was taken to be 7 Å (*31*, *32*). The nearest atom in the microenvironment to each atom of the indole or phenol ring was specified, and the distance between them was determined. For tyrosine residues, the neighbors of the OH group were also determined. The packing density of the atoms in a microenvironment was determined as the number of atoms comprising the microenvironment, or as the part of the microenvironment volume (V_0) occupied by the atoms ($d = \sum V_i/V_0$). The volume occupied by each atom (V_i) was determined according to its van der Waals radius, and only the part inside the microenvironment was taken into account. The real values of atom volume are slightly smaller, as atoms are incorporated in chemical bonds. Nonetheless, it is found to be not significant for the estimation of microenvironment packing density of tryptophan and tyrosine residues.

The efficiency of nonradiative energy transferred between any two chromophores was evaluated as follows (*33*):

$$W = \frac{1}{1 + \frac{2/3}{k^2}\left(\frac{R}{R_0}\right)^6} \quad (1)$$

where R_0 is the Förster distance, i.e., the average distance between a randomly orientated donor and acceptor at which $W = 0.5$; R is the distance between the geometrical centers of the indolic (or phenol) rings of a donor and an acceptor; and k^2 is the factor of mutual orientation of the donor and the acceptor.

$$k^2 = (\cos\theta - 3\cos\theta_A \cos\theta_D)^2 \quad (2)$$

where θ is the angle between the directions of the emission oscillator of a donor and the absorption oscillator of an acceptor, θ_A is the angle between the emission oscillator and the vector connecting the geometrical center of the donor, and θ_D is the angle between the absorption oscillator and the vector connecting the geometrical center of the acceptor (*34*). The values of R_0 for Trp-Trp, Tyr-Trp, and Tyr-Tyr pairs were taken from Eisenger et al. (*35*) and Steinberg (*36*). All other parameters were determined according to atoms coordinates (*31*, *32*, *37*). Oscillators were considered to be rigid in all calculations.

Fluorescence Measurements. All fluorescence experiments were carried out at 23 °C on a homemade steady-state spectrofluorimeter and pulse spectrofluorimeter for recording fluorescence decay curves (*38*). Fluorescence spectra were measured with excitation at 297 or 280 nm. The parameter A ($=I_{320}/I_{365}$, where I_{320} and I_{365} are the fluorescence intensity at 320 and 365 nm, respectively) was used for characterization of fluorescence spectra position (*37*). The fluorescence spectra and the values of parameter A were both corrected by the instrument sensitivity. The contribution of tyrosine residues to the bulk protein fluorescence was evaluated by the value

$$\Delta_\lambda = \left(\frac{I_\lambda}{I_{365}}\right)_{280} - \left(\frac{I_\lambda}{I_{365}}\right)_{297} \quad (3)$$

Analysis of Fluorescence Decay. The decay curves were analyzed in a multiexponential approach:

$$I(t) = \sum_i \alpha_i \exp(-t/\tau_i) \quad (4)$$

where α_i and τ_i are the amplitude and the lifetime of component i, respectively ($\sum\alpha_i = 1$).

The values of α_i and τ_i were determined from convolution of $I(t)$ with lamp impulse or reference decay curve. The fitting routine was based on the nonlinear least-squares method. Minimization was performed according to the method of Marquardt (*39*). P-Terphenyl in ethanol and *N*-acetyltryptophanamide in water were used as reference compounds (*40*).

The contribution of component i to the total emission S_i was calculated as

$$S_i = \frac{\alpha_i \int_0^\infty \exp(-t/\tau_i)\, dt}{\sum \alpha_i \int_0^\infty \exp(-t/\tau_i)\, dt} = \frac{\alpha_i \tau_i}{\sum \alpha_i \tau_i} \quad (5)$$

The root-mean square value of fluorescent lifetimes, $\langle\tau\rangle$, for biexponential decay is determined as

$$\langle\tau\rangle = \frac{\alpha_1 {\tau_1}^2 + \alpha_2 {\tau_2}^2}{\alpha_1\tau_1 + \alpha_2\tau_2} = \sum S_i \tau_i \quad (6)$$

Circular Dichroism Spectroscopy. Circular dichroism (CD) measurements were performed on homogeneous samples of GlnBP in 10 mM Tris-HCl buffer (pH 8.5) with a protein concentration of 0.2 mg/mL and specified amounts of glutamine. We used the J-710 spectropolarimeter (Jasco, Tokyo, Japan) equipped with the Neslab RTE-110 temperature-controlled liquid system (Neslab Instruments, Portsmouth, NH). The instrument was calibrated with a standard solution of (+)-10-camphorsulfonic acid. Sealed cuvettes with a path length of 0.1 cm (Helma, Jamaica, NJ) were used. The photomultiplier voltage never exceeded 600 V in the spectral regions that were measured. Each spectrum was averaged five times and smoothed with spectropolarimeter system software, version 1.00 (Jasco). All measurements were performed under a nitrogen flow. Before undergoing CD analyses, all samples were kept at the temperature being studied for 10 min. The results are expressed in terms of molar ellipticity (θ).

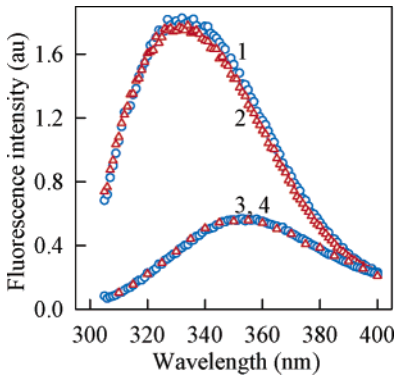

FIGURE 2: Fluorescence spectra of GlnBP and its complex with Gln in native (curves 1 and 2) and unfolded (curves 3 and 4) states. Denaturation was induced by 3.0 M GdnHCl; λ_{ex} = 297 nm. All values are reduced to the fluorescence intensity of native GlnBP at 365 nm.

RESULTS

In this work, the characteristics of GlnBP and GlnBP−Gln in native and unfolded states were examined and the equilibrium dependencies of different parameters of intrinsic fluorescence, intensity of ANS fluorescence, and CD in far- and near-UV spectra upon GdnHCl concentration were recorded.

Figure 2 shows the Trp emission spectra of GlnBP and GlnBP−Gln in native and unfolded (3.0 M GdnHCl) states upon excitation at 297 nm. The emission spectra appear to be smooth and featureless. The emission maximum is ~332 nm for the native GlnBP. It is slightly (1−2 nm) blue shifted upon Gln binding. As expected, protein unfolding by 3.0 M GdnHCl results in a significant red shift of the emission spectrum. Emission spectra of GlnBP and GlnBP with Gln in the presence of 3.0 M GdnHCl coincide, and the emission maximum of fluorescence spectra is 353 nm. The fluorescence intensity of the unfolded protein is significantly lower than that of the native one.

Figure 3 shows the tryptophan fluorescence decay curves of native and unfolded GlnBP. These curves for GlnBP−Gln were found to be practically the same as for GlnBP alone (data not presented). Table 1 lists the dependencies of the mean lifetimes of the excited states of GlnBP and GlnBP−Gln upon GdnHCl concentrations.

Figure 4A shows the contribution of tyrosine residues to the bulk fluorescence of native and unfolded GlnBP. Fluorescence spectra of the native protein excited at 280 nm only slightly differ from those obtained upon excitation at 297 nm. This suggests an insignificant contribution of tyrosine residues to the bulk emission of the native protein.

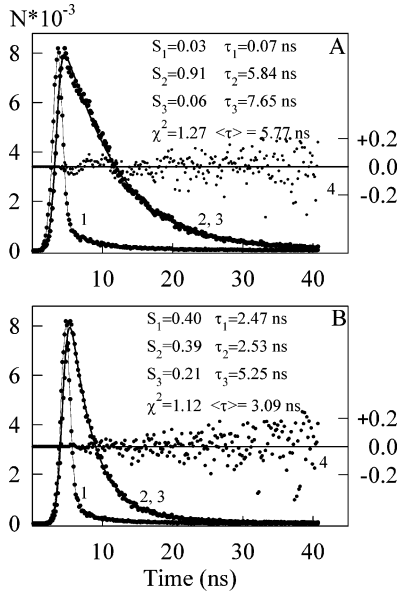

FIGURE 3: Decay curves of the tryptophan fluorescence of native (A) and unfolded (B) GlnBP. The symbols represent the excitation lamp profile (curve 1), the experimental decay curve (curve 2), the best fit calculated fluorescence decay curve (curve 3), and the deviation between the experimental and calculated decay curve (weighted residuals; curve 4). The excitation wavelength was 297 nm, and the registration wavelength was 340 nm. The fluorescence decay curves show the best fit with a three-exponential decay model. The values of τ_i, S_i, χ^2, and average lifetime $\langle\tau\rangle$ are shown.

Table 1: Lifetimes of the Excited States of GlnBP and GlnBP−Gln at Different GdnHCl Concentrations

	⟨τ⟩ (ns)	
[GdnHCl] (M)	GlnBP	GlnBP−Gln
0.0	5.77−5.85	5.78−5.59
0.5−1.3	4.18−4.26	5.71−5.59
3.0	3.00−3.07	3.08−3.12

On the other hand, the contribution of tyrosine residues in the unfolded protein is clearly revealed and significant. Figure 4B shows the change in the contribution of the tyrosine residues to the bulk fluorescence of GlnBP and GlnBP−Gln with the increase in GdnHCl concentration. The increase in tyrosine contribution starts at 0.2 M GdnHCl for GlnBP; it remains constant till 0.8 M GdnHCl for GlnBP−Gln. At 1.4 M GdnHCl, the second stage of the tyrosine contribution increase starts.

The GdnHCl-induced changes in several parameters of tryptophan fluorescence of GlnBP and GlnBP−Gln are given in Figure 5 which shows the variations of the fluorescence intensity recorded at 320 nm. This dependence of GlnBP suggests the existence of at least two transitions. The first transition lies in the range of 0.2−0.7 M GdnHCl, and the second one is in the range of 1.4−2.1 M GdnHCl. The same two transitions were recorded on the pathway of protein refolding. The values of fluorescence intensity recorded on the pathways of unfolding and refolding coincide. In contrast to GlnBP, the GdnHCl-induced changes in GlnBP−Gln fluorescence fit a two-state transition, which begins at 0.3 M GdnHCl and ends at 2.1 M GdnHCl.

Figure 5B shows the variations of the fluorescence intensity recorded at 365 nm. Contrary to the dependence of fluorescence intensity recorded at 320 nm, this dependence

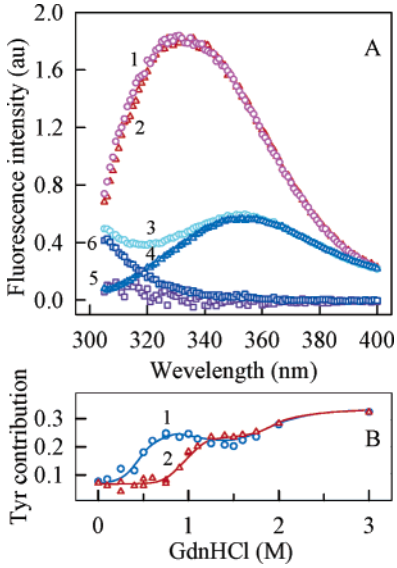

FIGURE 4: Contribution of tyrosine residues to the bulk fluorescence of the native and unfolded GlnBP. (A) Fluorescence spectrum of native (curves 1 and 2) and unfolded (curves 3 and 4) GlnBP excited at 280 nm (curves 1 and 3) and 297 nm (curves 2 and 4). Curves 1 and 2 are reduced to unity at 365 nm. Curves 3 and 4 are reduced to the fluorescence intensity of the native protein excited at 297 nm. Curves 5 and 6 represent the difference between curves 1 and 2 and between curves 3 and 4, respectively. (B) GdnHCl-induced unfolding of GlnBP in the absence (curve 1) and presence of Gln (curve 2) monitored as variations of the tyrosine contribution recorded at 320 nm (Δ_{320}).

has a pronounced increase in the range of 0.7−1.4 M GdnHCl, suggesting the complex character of this process.

Figure 5C shows the dependence of the fluorescence spectrum position represented by the parameter A (I_{320}/I_{365}). Protein unfolding is accompanied by a significant red shift of the fluorescent spectrum, i.e., decrease in parameter A. Like the curves of fluorescence intensity changes at 320 nm, the dependence of parameter A for GlnBP consists of two transitions. The first transition lies in the range of 0.2−0.7 M GdnHCl, and the second is in the range of 1.4−2.1 M GdnHCl. The curves of protein refolding coincide with those of protein unfolding. For GlnBP−Gln, the GdnHCl-induced change in parameter A fits a two-state transition. The transition begins at 1.3 M GdnHCl and ends at 2.1 M GdnHCl.

Figure 5E shows the GdnHCl-induced change in fluorescence anisotropy. Contrary to the fluorescence intensity and fluorescence spectrum position, the dependencies of fluorescence anisotropy for GlnBP and GlnBP−Gln coincide from 0.0 to 3.0 M GdnHCl. The value of the fluorescence anisotropy remains constant till 1.3−1.4 M GdnHCl for both GlnBP and GlnBP−Gln. In the range of 1.4−2.0 M, it sharply decreases, reaching the value characteristic of the unfolded protein at 3.0 M GdnHCl.

The fluorescence of ANS added to solutions of GlnBP and GlnBP−Gln containing different GdnHCl concentration was recorded at 480 nm (λ_{ex} = 365 nm). The data are given in Figure 5F. For both GlnBP and GlnBP−Gln, these dependencies are represented by bell-shaped curves. The value of fluorescence intensity of ANS in solutions of the native protein (in the presence of 0.0 M GdnHCl) and completely unfolded one (in the presence of 3.0 M GdnHCl) is very low and practically identical to the value of free ANS

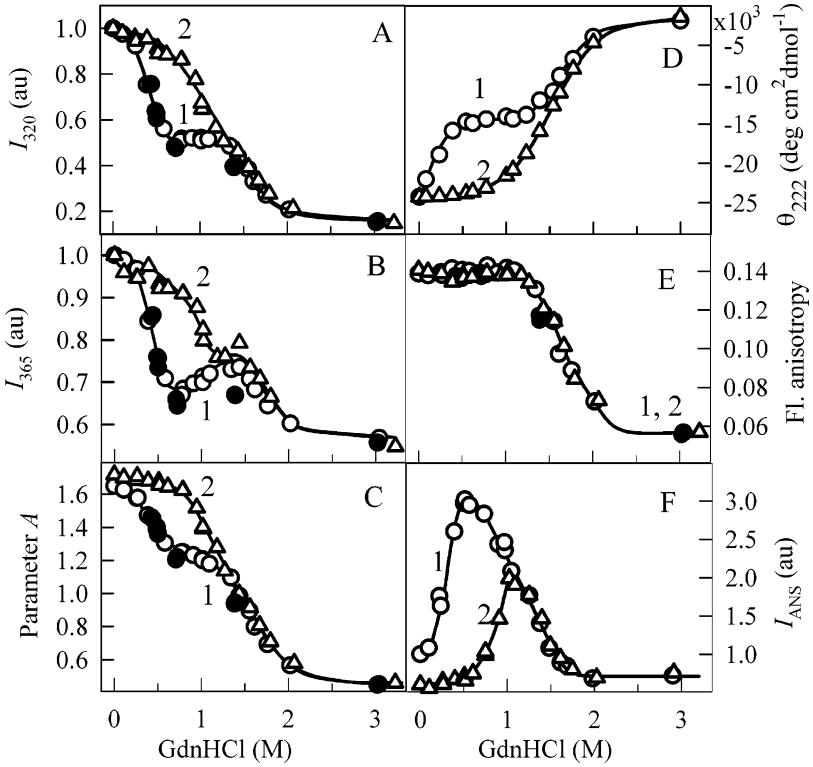

FIGURE 5: GdnHCl-induced conformational transitions of GlnBP (curve 1) and its complex with Gln (curve 2). (A) Change in fluorescence intensity at 320 nm; $\lambda_{ex} = 297$ nm. (B) Change in fluorescence intensity at 365 nm; $\lambda_{ex} = 297$ nm. (C) Change in parameter A ($=I_{320}/I_{365}$); $\lambda_{ex} = 297$ nm. (D) Change in the ellipticity at 222 nm. (E) Change in the fluorescence anisotropy; $\lambda_{ex} = 297$ nm, and $\lambda_{em} = 365$ nm. (F) Change in the ANS fluorescence intensity; $\lambda_{ex} = 365$ nm, and $\lambda_{em} = 480$ nm. Data for unfolding are depicted with empty symbols and data for refolding with filled ones.

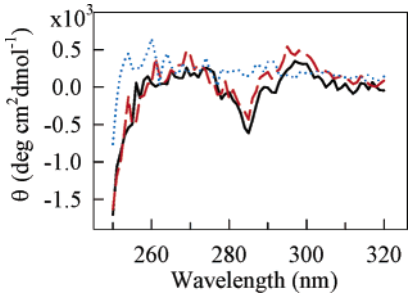

FIGURE 6: Near-UV CD spectra of GlnBP. Solid, dashed, and dotted curves correspond to 0.0, 0.75, and 3.0 M GdnHCl, respectively.

under the same conditions. For GlnBP, the increase in ANS fluorescence intensity starts at a very low GdnHCl concentration (0.1 M), reaching a maximum at ~0.5 M GdnHCl, and then it decreases, reaching a plateau at 1.6 M. For GlnBP−Gln, the start of the increase in the ANS intensity emission and emission maximum of the curve is shifted to higher GdnHCl concentrations (0.5 and 1.2 M, respectively). The descending part of the curve coincides with that for GlnBP.

The GdnHCl-induced unfolding of GlnBP was also characterized by far- and near-UV CD. Figure 5D shows the dependence of the protein ellipticity at 222 nm on GdnHCl concentration. Figure 6 shows the near-UV CD spectra of GlnBP recorded in the presence of 0.0, 0.75, and 3.0 M GdnHCl.

DISCUSSION

The equilibrium dependencies of intrinsic fluorescence, intensity fluorescence of ANS, and CD in far- and near-UV regions of GlnBP and its complex with Gln on GdnHCl concentration were recorded to study the processes of their unfolding and refolding. The data obtained by intrinsic fluorescence were analyzed taking into account the properties of microenvironments and peculiarities of localization of tryptophan and tyrosine residues in the protein (*41*).

Tryptophan Fluorescence of GlnBP. The emission maximum of native GlnBP was recorded at ~332 nm. These data differ from those obtained earlier by Weiner and Heppel (*42*), who recorded the emission maximum of 336 nm by excitation at 280 nm, but are comparable to that of Axelsen et al. (*43*), who recorded the emission maximum of 330 nm by excitation at 295 nm. The unfolding of GlnBP macromolecules induced by 3.0 M GdnHCl is accompanied by a red shift of the tryptophan fluorescence spectrum and by a significant decrease in fluorescence intensity (Figure 2).

Analysis of the 3D structure of the GlnBP (PDB entry 1GGG; *16*, *18*) showed that both tryptophan resides of this protein (Trp 32 and Trp 220) are located in the large domain far from ligand-binding site. Trp32 is in the first α-helix (Phe 27−Glu 38), and Trp 220 is in the final one (Thr 212−Phe 221). Tryptophan residues are located far from each other ($R = 16$ Å), and the efficiency of energy transfer between them is negligible. Their microenvironment density is not very high (there are 63 atoms and 66 atoms in the microenvironments of Trp 32 and Trp 220, respectively), and both tryptophan residues are partially accessible to solvent. The polarity of their microenvironments differs significantly. There are many hydrophobic groups (Leu 5, Val 7, Ile 35, Ala 36, Leu 39, Leu 41, ring of Tyr 43, Leu 45, Leu 64, Leu 66, Ile 187, and Val 200) and only one polar group of

the amino acid side chain (OH group of Tyr 43) in the microenvironment of Trp 32. In the microenvironment of Trp 220, there are four polar groups of the side chains of amino acids (Asp 30, Tyr 163, Lys 166, and Lys 219) and only seven nonpolar groups (Pro 15, Phe 18, Val 25, Phe 27, Tyr 163, Ile 216, and Phe 221) which is essentially fewer than in the vicinity of Trp 32. So it is likely that the fluorescence spectrum of Trp 220 is more red shifted in comparison with that of Trp 32, which agrees with the conclusions of Axelsen et al. (*43*).

The fluorescence decay curves show the best fit with a three-exponential decay model with an average lifetime of the native protein of 5.77 ns that is in good agreement with the data of Axelsen et al. (*43*). The fluorescence lifetime of the unfolded protein (3.09 ns) is similar to that of other denatured proteins (*44*). The GdnHCl-induced decrease in both the fluorescence lifetime and the tryptophan fluorescence intensity suggests an increase in the extent of fluorescence dynamic quenching on protein unfolding.

The equilibrium dependencies of tryptophan fluorescence intensity and fluorescence spectrum position revealed two transitions (Figure 5A,C). Usually the shift in the fluorescence spectrum is characterized by the change in its maximum, yet it is difficult accurately to determine the maximum of a wide smooth spectrum as it is the fluorescence spectrum of GlnBP. So to this end, we used the ratio of fluorescence intensities on the slopes of the emission spectrum ($A = I_{320}/I_{365}$), which characterizes fluorescence shift more precisely. This characteristic is very sensitive to the shifts in the fluorescence spectrum because the spectrum shift results in opposite sign fluorescence intensity changes on the different slopes (*37*, *38*). The obtained dependencies of parameter *A* upon GdnHCl concentration suggest that the first transition starts at a very low GdnHCl concentration (0.2 M) and ends at 0.7 M GdnHCl, and the second transition which apparently corresponds to unfolding of protein structure begins at 1.4 M GdnHCl and ends at 2.1 M GdnHCl.

Contrary to the fluorescence intensity and fluorescence spectrum position, fluorescence anisotropy remains constant up to 1.4 M GdnHCl, i.e., till the beginning of the second transition. One can suggest that in the range from 0.0 to 1.4 M GdnHCl the protein preserves a globular structure with the microenvironment of the tryptophan residues that restricts the indole ring intramolecular mobility. This assumption does not contradict the fluorescence spectrum position and near-UV CD data. When relaxation properties of protein structure are being evaluated, it is necessary to distinguish between the mobility of the microenvironment of tryptophan residues and the mobility of indole rings themselves. The information about the mobility of the tryptophan residue microenvironment could be obtained from the position of the fluorescence spectrum and from the near-UV CD spectrum, while the value of their fluorescence anisotropy gives the information about the mobility of tryptophan residues themselves. Earlier, we showed that a pronounced red shift in the tryptophan fluorescence spectrum does not necessarily reflect the considerable increase in its environment mobility (*45*, *46*). Furthermore, the red shift of the tryptophan fluorescence spectrum can be accompanied by an increase in fluorescence anisotropy (*37*, *47*).

Yet, there can be another more trivial explanation of this phenomenon. One can suggest superposition of two opposite effects on the value of tryptophan fluorescence anisotropy: the increase in the mobility of tryptophan residues, which is accompanied by the decrease in fluorescence anisotropy, and the decrease in fluorescence lifetime (Table 1), which is accompanied by the increase of fluorescence anisotropy. The significant disruption of the secondary structure of GlnBP in 0.1−0.6 M GdnHCl that is suggested by the data of far-UV CD (Figure 5D) proves the assumption that partially unfolding GlnBP in this range of GdnHCl concentrations is accompanied by the increase in the mobility of of tryptophan residues.

Tyrosine Fluorescence of GlnBP. Usually the use of protein intrinsic fluorescence implies its tryptophan fluorescence. This is due to the high sensitivity of all tryptophan fluorescence characteristics to their microenvironment. However, there is risk in monitoring only local structural changes using trytophan fluorescence. That is why along with tryptophan fluorescence, the recording of that of tyrosine could also be useful. As opposed to trytophan residues, usually there are many tyrosine residues in proteins. In GlnBP, there are two tryptophan and 10 tyrosine residues; four tyrosine residues are located in the small domain, and the other six are in the large domain (Figure 1). Though not all parameters of tyrosine fluorescence are sensitive to their microenvironment, the advantage of monitoring their fluorescence is that they are located all over the protein macromolecule, and there is a chance of finding some other transitions in protein unfolding.

Though GlnBP contains 10 tyrosine residues, their contribution to the bulk fluorescence of native GlnBP is negligible. Analysis of the microenvironments of tyrosine residues showed that there are two reasons for their low quantum yield in GlnBP. First, there are conditions for effective energy transfer from the majority of tyrosine to tryptophan residues. All tyrosine residues except Tyr 123 can effectively transfer their excitation energy directly to Trp 32 and/or Trp 220, or via other Tyr residues. Second, most of the tyrosine residues could be quenched not only by energy transfer to tryptophan residues but also by quenching groups in their vicinity or by effective energy transfer to tyrosine residues which are quenched.

However, tyrosine fluorescence intensity increases significantly when GlnBP is unfolded in 3.0 M GdnHCl (Figure 4A). The change in the contribution of tyrosine residues to the bulk fluorescence of protein can be regarded as a parameter for monitoring protein unfolding. The dependence of the contribution of tyrosine residues to the protein bulk fluorescence on GdnHCl concentration (Figure 4B) confirms the existence of at least two transitions in the process of GlnBP unfolding.

To characterize the partially unfolded transition state of GlnBP, the binding of hydrophobic fluorescence dye ANS was examined (Figure 5F). The significant increase in ANS fluorescence in the range of the first transition ($N \rightarrow I_1$), revealed by the fluorescence intensity and fluorescence spectrum position, could be connected with the existence of a molten globule-like state. This assumption, however, contradicts the data of the far-UV CD spectrum, which suggests the disorder of secondary structure of GlnBP as the result of the $N \rightarrow I_1$ transition.

Despite the complex character of GlnBP denaturation, it was found to be reversible. The decrease in GdnHCl

concentration from 3.0 to 1.38, 0.71, 0.50, and 0.43 M by solution dilution induces the restoration of the protein fluorescence characteristics to values that are typical for these GdnHCl concentrations on the pathway of protein denaturation (Figure 5A−C,E).

Examination of Folding and Unfolding of Proteins by the Parametric Representation of the Relation between Two Independent Extensive Characteristics of the System. For a more detailed analysis of the GlnBP unfolding process and to determine the number of intermediate states that appear on the pathway from the native to unfolded protein, we used the method of phase diagrams (*27*, *28*, *48*, *49*). This method implies the construction of parametric dependencies of two independent extensive parameters of the system. Any extensive characteristic of a system consisting of two components is determined by the simple equation

$$I(\theta) = \alpha_1(\theta)I_1 + \alpha_2(\theta)I_2 \quad (7)$$

where I_1 and I_2 are the values of $I(\theta)$ at 100% content of the first and second components, respectively, and $\alpha_1(\theta)$ and $\alpha_2(\theta)$ are the relative fractions of the components in the system, $\alpha_1(\theta) + \alpha_2(\theta) = 1$, where θ is any parameter depending on which of the components is changed. The denaturant concentration, temperature, pH of the solution, etc., can be taken as a parameter. Only for extensive characteristics which give quantitative characterization of the system is eq 7 valid, and the fraction of the components in the system, as well as the equilibrium constant K, can be determined by simple equations:

$$\alpha_1(\theta) = \frac{I(\theta) - I_2}{I_1 - I_2},\ \alpha_2(\theta) = \frac{I_1 - I(\theta)}{I_1 - I_2},\ K(\theta) = \frac{I_1 - I(\theta)}{I(\theta) - I_2} \quad (8)$$

If intensive characteristics [such as fluorescence spectrum position, parameter A (*37*), fluorescence anisotropy, etc., which characterize the system qualitatively] are used, these equations for determination of $\alpha_1(\theta)$, $\alpha_2(\theta)$, and $K(\theta)$ are not valid (*25*, *26*), though often no account is taken of this in the investigations of protein conformation transitions. For any two independent extensive characteristics, we have

$$I_1(\theta) = \alpha_1(\theta)I_{1,1} + \alpha_2(\theta)I_{2,1} \quad (9)$$

and

$$I_2(\theta) = \alpha_1(\theta)I_{1,2} + \alpha_2(\theta)I_{2,2} \quad (10)$$

Eliminating $\alpha_1(\theta)$ and $\alpha_2(\theta)$ from eqs 9 and 10, we can obtain the relationship between $I_1(\theta)$ and $I_2(\theta)$:

$$I_1(\theta) = a + bI_2(\theta) \quad (11)$$

where $a = I_{1,1} - [(I_{2,1} - I_{1,1})/(I_{2,2} - I_{1,2})]I_{1,2}$ and $b = (I_{2,1} - I_{1,1})/(I_{2,2} - I_{1,2})$.

Equation 11 means that if with the change in parameter θ the transition between states 1 and 2 follows the model of a two-state transition without formation of the intermediate states, then the parametric relationship between any two extensive characteristics must be linear. If the experimentally recorded parametric relationship between two extensive characteristics of the system is not linear, it unequivocally means that the process of the transition from the initial to the final state is not a one-stage process but proceeds with the formation of one or several intermediate states. This approach has been used for characterization of intermediate states of a number of proteins (*27*, *29*, *48*, *49*).

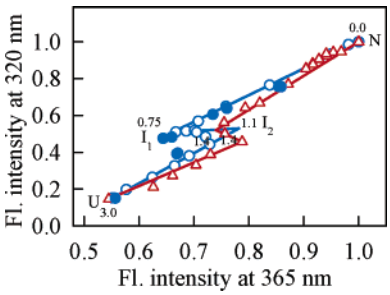

FIGURE 7: Parametric relationships between I_{320} and I_{365}, characterizing GdnHCl-induced unfolding of GlnBP (blue ○) and its complex with Gln (red △), where the parameter is GdnHCl concentration. Filled circles represent the results of GlnBP refolding. The fluorescence characteristics corresponding to native (N), intermediate (I_1 and I_2), and completely unfolded (U) states are indicated. The values on the curves are the values of GdnHCl concentrations.

The character of the parametric relationship between I_{320} and I_{365} with GdnHCl concentration taken as a parameter suggests the existence of two successively appearing intermediate states (I_1 and I_2) on the pathway of the GlnBP transition from the native to completely unfolded state (Figure 7):

$$N \rightleftarrows I_1 \rightleftarrows I_2 \rightleftarrows U \quad (12)$$

The $N \rightleftarrows I_1$ transition occurred in the range of GdnHCl concentrations from 0.0 to 0.6−0.7 M for GlnBP. This transition is accompanied by a decrease in fluorescence intensity (Figure 5A), the decrease in parameter A (Figure 5C), the increase in the contribution of tyrosine to the bulk protein fluorescence (Figure 4B), and the increase in fluorescence intensity of ANS (Figure 5F). The invariance of the value of the protein fluorescence anisotropy up to 1.1 M GdnHCl suggests that in this range of GdnHCl concentrations the protein preserves a globular and rather rigid structure despite the significant decrease in the far-UV CD signal (see above).

The $I_1 \rightleftarrows I_2$ transition became evident in the equilibrium dependence of fluorescence intensity recorded at 365 nm (Figure 5B) and in parametric dependencies (see Figure 7). Furthermore, for GlnBP the existence of I_2 can be seen from the comparison of the equilibrium dependencies of fluorescence anisotropy r and the intensity of ANS fluorescence upon GdnHCl concentration (Figure 5E,F). The increase in the intensity of ANS fluorescence corresponds to the $N \rightarrow I_1$ transition. The intensity of ANS fluorescence begins to decrease earlier than the complete unfolding of protein, which is reflected in the decrease in fluorescence anisotropy. It is reasonable to assume the existence of the extra transition ($I_1 \rightarrow I_2$) accompanying by the diminishing of ANS fluorescence intensity which precedes the complete protein unfolding ($I_2 \rightarrow U$). The $I_1 \rightarrow I_2$ transition takes place in the range of 0.75−1.1 M GdnHCl. At the same time, neither the dependence of fluorescence intensity at 320 nm nor the dependence of parameter A suggests any transition in this range of GdnHCl concentrations. According to far-UV CD

data, the secondary structure is also unchanged in this range of GdnHCl concentrations (Figure 5D).

The $I_2 \rightleftarrows U$ transition takes place when the GdnHCl concentration is in the range of 1.1−2.4 M. As a result of this transition, the compact globular structure is destroyed. First of all, it is visualized in the dramatic shift of the fluorescence spectrum, i.e., in the decrease of parameter *A* (Figure 5C), that suggests the increase in the polarity of the tryptophan residue microenvironment. The decrease in fluorescence anisotropy in this range of GdnHCl concentrations (Figure 5E) suggests the increase in the mobility of tryptophan residues and their microenvironment. This is also evident from the change in the near-UV CD spectrum (Figure 6). The significant decrease in the ellipticity at 222 nm (Figure 5D) indicates the destruction of the secondary structure of protein in this transition. Interestingly, the decrease in the fluorescence intensity of ANS begins at GdnHCl concentrations which are essentially lower than that at which the $I_2 \rightleftarrows U$ transition begins. This indirectly suggests the existence of the I_2 state. It means also that when the protein is transferred to the I_2 state it loses the ability to bind ANS.

GlnBP is a two-domain protein, and we cannot avoid the possibility that the domain unfolds successively. At the same time, the $N \rightarrow I_1$ transition cannot be explained by unfolding of a small domain (which has no Trp), as it is accompanied by a significant change in fluorescence characteristics. In the work of D'Auria et al. (*50*), a lower thermal sensitivity of the protein α-helices than *β*-sheets is shown by FTIR. Maybe it also takes place when the protein is unfolded by GdnHCl. In this sense, it is important that thermal denaturation (as opposed to unfolding induced by GdnHCl) never completely unfolds proteins. Thus, we can assume that in our case the $N \rightarrow I_1$ process is accompanied by unfolding of α-helices, while the $I_1 \rightarrow I_2$ transition is connected with destruction of *β*-sheets.

Unfolding and Refolding of the Complex of GlnBP with Gln. GlnBP Stabilization by Ligand Binding. The binding of L-glutamine causes cleft closing and a significant structural change with the formation of the so-called closed form structure (Figure 1, PDB entry 1WND; *17*). Nonetheless, Gln binding induces insignificant changes in the microenvironments of Trp 32 and Trp 220. In GlnBP−Gln, there are 65 atoms in the microenvironments of both tryptophan residues. As mentioned above, the only polar group in the vicinity of Trp 32 is the OH group of Tyr 43. The position of this group changes only slightly with the formation of GlnBP−Gln. Although the number of atoms in the microenvironment of Trp 220 is practically the same for ligand-free and ligand-bound GlnBP, its composition undergoes some change. In the Trp 220 microenvironment of GlnBP are Pro 15, Phe 18, Phe 27, Phe 221, and Tyr 163, while in GlnBP−Gln, only Pro 15, Phe 18, and Phe 27 remain in the microenvironment. Phe 221 and Tyr 163 which belong to the other domain leave the microenvironment of Trp 220 when this domain turns upon formation of the complex. There are more polar groups in the microenvironment of Trp 220 in the absence of the ligand (six) than in the complex with Gln (four). When the complex is formed, the OH group of Tyr 163 and N2 of Lys 166 are removed from the microenvironment, while the positions of other groups are changed only slightly (Figure 1). All this explains why ligand binding does not significantly change the tryptophan fluorescence spectrum of GlnBP (Figure 2). The results obtained by FTIR (*50*) show that binding of Gln induces only small changes in the secondary structure of the protein. In this work, it is also shown that Gln binding renders the structure of GlnBP more thermostable.

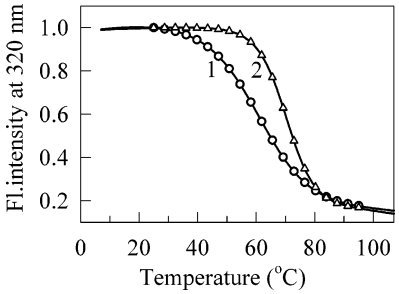

FIGURE 8: Temperature-induced unfolding of GlnBP and GlnBP−Gln. Curves 1 and 2 represent the changes in fluorescence intensity at 320 nm of GlnBP and GlnBP−Gln, respectively; $\lambda_{ex} = 297$ nm.

Our data suggest that the structure of GlnBP in the presence of Gln is not only more thermostable (Figure 8) but also much more resistant to the denaturing action of GdnHCl. In fact, for GlnBP−Gln, the $N \rightleftarrows I_1$ transition occurs at a higher concentration of GdnHCl (Figure 5A−D,F). It means that $N \rightleftarrows I_1$, $I_1 \rightleftarrows I_2$, and $I_2 \rightleftarrows U$ processes pass through a more narrow range of GdnHCl concentrations. Due to Gln binding, protein unfolding becomes more cooperative and it resists higher concentrations of GdnHCl. It causes the illusion that the process of GlnBP−Gln unfolding includes one intermediate state. Nonetheless, the character of the parametric relationship between I_{320} and I_{365} (Figure 7) uniquely shows that the process of the unfolding of GlnBP−Gln is also a three-stage process as it is for GlnBP.

REFERENCES

1. Arai, M., and Kuwajima, K. (2000) Role of the molten globule state in protein folding, *Adv. Protein Chem. 53*, 209−282.
2. Bilsel, O., and Matthews, C. R. (2000) Barriers in protein folding reactions, *Adv. Protein Chem. 53*, 153−207.
3. Dinner, A. R., Sali, A., Smith, L. J., Dobson, C. M., and Karplus, M. (2000) Understanding protein folding via free-energy surfaces from theory and experiment, *Trends Biochem. Sci. 25*, 331−339.
4. Dobson, C. M. (2003) Protein folding and misfolding, *Nature 426*, 884−890.
5. Grantcharova, V., Alm, E. J., Baker, D., and Horwich, A. L. (2001) Mechanisms of protein folding. *Curr. Opin. Struct. Biol. 11*, 70−82.
6. Jaenicke, R., and Lilie, H. (2000) Folding and association of oligomeric and multimeric protein, *Adv. Protein Chem. 53*, 329−401.
7. Kim, P. S., and Baldwin, R. L. (1990) Intermediates in the folding reactions of small proteins, *Annu. Rev. Biochem. 59*, 631−660.
8. Plotkin, S. S., and Onuchic, J. N. (2002) Understanding protein folding with energy landscape theory. Part I: Basic concepts, *Q. Rev. Biophys. 35*, 111−167.
9. Ptitsyn, O. B. (1995) Molten globule and protein folding, *Adv. Protein Chem. 47*, 83−229.
10. Radfod, S. (2000) Protein folding: Progress made and promises ahead, *Trends Biochem. Sci. 25*, 611−618.
11. Fink, A. L. (1998) Protein aggregation: Folding aggregates, inclusion bodies and amyloid, *Folding Des. 3*, R9−R23.
12. Wetzel, R. (1994) Mutations and off-pathway aggregation of proteins, *Trends Biotechnol. 12*, 193−198.
13. Carrell, R. W., and Gooptu, B. (1998) Conformational changes and disease: Serpins, prions and Alzheimer's, *Curr. Opin. Struct. Biol. 8*, 799−809.

14. Harper, J. D., and Lansbury, P. T., Jr. (1997) Models of amyloid seeding in Alzheimer's disease and scrapie: Mechanistic truths and physiological consequences of the time-dependent solubility of amyloid proteins, *Annu. Rev. Biochem. 66*, 385−407.
15. Speed, M. A., Wang, D. I., and King, J. (1996) Specific aggregation of partially folded polypeptide chains: The molecular basis of inclusion body composition, *Nat. Biotechnol. 14*, 1283−1287.
16. Hsiao, C.-D., Sun, Y.-J., Rose, J., and Wang, B.-C. (1996) The crystal structure of glutamine-binding protein from *Escherichia coli*, *J. Mol. Biol. 262*, 225−242.
17. Sun, Y. J., Rose, J., Wang, B. C., and Hsiao, C. D. (1998) The structure of glutamine-binding protein complexed with glutamine at 1.94 Å resolution: Comparisons with other amino acid binding proteins, *J. Mol. Biol. 278*, 219−229.
18. Bernstein, F. C., Koetzle, T. F., Williams, G. J. B., Meyer, E. F., Jr., Brice, M. D., Rodgers, J. R., Kennard, O., Shimanouchi, T., and Tasumi, M. (1977) The Protein Data Bank: A computer-based archival file for macromolecular structures, *J. Mol. Biol. 112*, 535−542.
19. Humphrey, W., Dalke, A., and Schulten, K. (1996) VMD: Visual molecular dynamics, *J. Mol. Graphics 14*, 33−38.
20. Merritt, E. A., and Bacon, D. J. (1977) Raster3D: Photorealistic molecular graphics, *Methods Enzymol. 277*, 505−524.
21. Dattelbaum, J. D., and Lakowicz, J. R. (2001) Optical determination of glutamine using a genetically engineered protein, *Anal. Biochem. 291*, 89−95.
22. D'Auria, S., and Lakowicz, J. R. (2001) Enzyme fluorescence as a sensing tool: New perspectives in biotechnology, *Curr. Opin. Biotechnol. 12*, 99−104.
23. Bychkova, V. E., and Ptitsyn, O. B. (1993) The molten globule in vitro and in vivo, *Chemtracts: Biochem. Mol. Biol. 4*, 133−163.
24. Lakowicz, J. R. (1999) *Principles of Fluorescence Spectroscopy*, 2nd ed., Kluwer Academic/Plenum Publishers, New York.
25. Eftink, M. R. (1994) The use of fluorescence methods to monitor unfolding transitions in proteins, *Biophys. J. 66*, 482−501.
26. Eftink, M. R. (1998) The use of fluorescence methods to monitor unfolding transitions in proteins, *Biokhimiya 63*, 327−337.
27. Kuznetsova, I. M., Stepanenko, O. V., Stepanenko, O. V., Povarova, O. I., Biktashev, A. G., Verkhusha, V. V., Shavlovsky, M. M., and Turoverov, K. K. (2002) The place of inactivated actin and its kinetic predecessor in actin folding-unfolding, *Biochemistry 41*, 13127−13132.
28. Stepanenko, O. V., Kuznetsova, I. M., Turoverov, K. K., Chunjuan, H., and Wang, C.-C. (2004) Conformational change of dimeric DsbC molecule induced by GdnHCl: A study by intrinsic fluorescence, *Biochemistry 43*, 5296−5303.
29. Bushmarina, N. A., Kuznetsova, I. M., Biktashev, A. G., Turoverov, K. K., and Uversky, V. N. (2001) Partially folded conformations in the folding pathway of bovine carbonic anhydrase II: A fluorescence spectroscopic analysis, *ChemBioChem 2*, 813−821.
30. Bradford, M. M. (1976) A rapid and sensitive method for the quantization of microgram quantities of protein utilizing the principle of protein-dye binding, *Anal. Biochem. 72*, 248−254.
31. Turoverov, K. K., Kuznetsova, I. M., and Zaitzev, V. N. (1985) The environment of the tryptophan residue in *Pseudomonas aeruginosa* azurin and its fluorecsence properties, *Biophys. Chem. 23*, 79−89.
32. Kuznetsova, I. M., and Turoverov, K. K. (1998) What determines the characteristics of protein intrinsic fluorescence? Analysis of tryptophan residue localization in proteins, *Tsitologia 40*, 747−762.
33. Forster, Th. (1960) Transfer mechanisms of electronic excitation energy, *Radiat. Res., Suppl. 2*, 326−339.
34. Dale, R. E., and Eisinger, J. (1974) Intramolecular distances determined by energy transfer. Dependence on orientational freedom of donor and acceptor, *Biopolymers 13*, 1573−1605.
35. Eisinger, J., Feuer, B., and Lamola, A. A. (1969) Intramolecular singlet excitation transfer. Applications to polypeptides, *Biochemistry 8*, 3908−3915.
36. Steinberg, I. Z. (1971) Long-range nonradiative transfer of electronic excitation energy in proteins and polypeptides, *Annu. Rev. Biochem. 40*, 83−114.
37. Turoverov, K. K., and Kuznetsova, I. M. (2003) Intrinsic fluorescence of actin, *J. Fluoresc. 13*, 41−57.
38. Turoverov, K. K., Biktashev, A. G., Dorofeyuk, A. S., and Kuznetsova, I. M. (1998) Device and program for investigations of spectral, polarizational and kinetic characteristics of fluorescence in solution, *Tsitologia 40*, 806−817.
39. Marquardt, D. W. (1963) An algorithm for least-squares estimation of nonlinear parameters, *J. Soc. Ind. Appl. Math. 11*, 431−441.
40. Zuker, M., Szabo, A. G., Bramall, L., Krajcarski, D. T., and Selinger, B. (1985) The delta function convolution method (DFCM) for fluorescence decay experiments, *Rev. Sci. Instrum. 56*, 14−22.
41. Kuznetsova, I. M., Stepanenko, O. V., Turoverov, K. K., Staiano, M., Scognamiglio, V., Rossi, M., and D'Auria, S. (2005) Fluorescence properties of glutamine-binding protein from *Escherichia coli* and its complex with glutamine, *J. Proteome Res. 4* (in press).
42. Weiner, J. H., and Heppel, L. A. (1971) A binding protein for glutamine and its relation to active transport in *E. coli*, *J. Biol. Chem. 246*, 6933−6941.
43. Axelsen, P. H., Bajzer, Z., Prendergast, F. G., Cottam, P. F., and Ho, C. (1991) Resolution of fluorescence intensity decays of the two tryptophan residues in glutamine-binding protein from *Escherichia coli* using single tryptophan mutants, *Biophys. J. 60*, 650−659.
44. Grinvald, A., and Steinberg, I. Z. (1976) The fluorescence decay of tryptophan residues in native and denatured proteins, *Biochim. Biophys. Acta 427*, 663−678.
45. Kuznetsova, I. M., and Turoverov, K. K. (1983) Polarization of intrinsic fluorescence of proteins. III. Intramolecular mobility of tryptophan residues, *Mol. Biol.* (*Moscow*) *17*, 741−754.
46. Turoverov, K. K., and Kuznetsova, I. M. (1998) What determines the characteristics of protein intrinsic fluorescence? Analysis of tryptophan residue localization in proteins, *Tsitologia 40*, 735−746.
47. Turoverov, K. K., Bictashev, A. G., Khaitlina, S. Yu., and Kuznetsova, I. M. (1999) The structure and dynamics of partially-folded actin, *Biochemistry 38*, 6261−6269.
48. Kuznetsova, I. M., Stepanenko, O. V., Turoverov, K. K., Zhu, L., Zhou, J.-M., Fink, A. L., and Uversky, V. N. (2002) Unraveling multistate unfolding of rabbit muscle creatine kinase, *Biochim. Biophys. Acta 1596*, 138−155.
49. Kuznetsova, I. M., Turoverov, K. K., and Uversky, V. N. (2004) Use of the phase diagram method to analyze the protein unfolding-refolding reactions: Fishing out the "invisible" intermediates, *J. Proteome Res. 3*, 485−494.
50. D'Auria, S., Scire, A., Varriale, A., Scognamiglio, V., Staiano, M., Ausili, A., Marabotti, A., Rossi, M., and Tanfani, F. (2005) Binding of glutamine to glutamine-binding protein from *Escherichia coli* induces changes in protein structure and increases protein stability, *Proteins: Struct., Funct., Bioinf. 58*, 80−87.

BI0478300